Desalination and Water Treatment
www.deswater.com

doi: 10.5004/dwt.2021.26888

217 (2021) 221–231
March

Adsorption behavior of Cr(VI) on activated carbon: isotherm, kinetic, and thermodynamic studies

Esra Altintig[a,*] Mehtap Karakas[b], Nilgun Basok[b], Hüseyin Altundag[c]

[a] *Sakarya University of Applied Sciences, Pamukova Vocational School, 54055 Sakarya, Turkey, email: altintig@subu.edu.tr*
[b] *Sakarya Saski, Wastewater Treatment Branch Directorate, Water and Wastewater Control Laboratory, 54030 Sakarya, Turkey, emails: mehtapkarakas1@hotmail.com (M. Karakas), nilgunbasok@gmail.com (N. Basok)*
[c] *Art and Science Faculty, Chemistry Department, Sakarya University, 54187 Sakarya, Turkey, email: altundag@sakarya.edu.tr*

Received 23 June 2020; Accepted 1 December 2020

ABSTRACT

In this study, the removal of Cr(VI) with activated carbon obtained by activation of chestnut inner shells with H_3PO_4 agricultural waste, was examined. The effect of different parameters such as initial pH to adsorption (1.0–8.0), initial Cr(VI) concentration (25–250 mg L^{-1}), amount of adsorbent (0.05–1.0 g 100 mL^{-1}), temperature (293–313 K), and contact time (5–120 min), were examined. As a result of experimental studies, the highest Cr(VI) removal was identified as 60 min. The highest yield of Cr(VI) was obtained at pH 2.0. The adsorption capacity of activated carbon is 227.27 mg g^{-1}. According to the obtained experimental data, it was observed that the equilibrium adsorption was consistent with the Langmuir isotherm. Kinetic studies have determined that Cr(VI) adsorption is the pseudo-second-order. The thermodynamic parameters calculated to estimate the nature of adsorption indicated a spontaneous and endothermic adsorption. All experimental results showed that the environmentally friendly, low-cost, and easily available adsorbent for the removal of Cr(VI) ion from aqueous solution by activated carbon obtained with activation of chestnut inner shells with H_3PO_4.

Keywords: Activated carbon; Chromium(VI); Adsorption; Thermodynamic; Kinetic

---

1. Introduction

In recent years, heavy metals have attracted considerable attention due to their toxic and carcinogenic effects to humans and aquatic organisms. Chromium and its derivatives, which are widely used in the industry, have negative effects on water quality. Chromium is derived as a result of activities such as metal coating, metal cutting, leather tanning, paint and pigment production, mining, and ore processing [1]. Chromium is present in two different oxidation loads, Cr(III) and Cr(VI) in natural waters. While Cr(III) is more stable and less toxic to living organisms and animals, Cr(VI) is mutagenic and carcinogenic in living organisms [2]. Cr(VI) is usually found in waters as chromate (CrO_4^{-2}) or dichromate ($Cr_2O_7^{-2}$) ions [3]. According to WHO, the maximum allowable limit for Cr(VI) is 0.05 mg L^{-1} [4]. Therefore, heavy metals such as chromium must be removed from these environments. General treatment techniques applied to pollution-containing wastewater include chemical precipitation, chemical oxidation, electrochemical processes, reverse osmosis [5,6] vacuum evaporation, membrane technologies, ion exchange, adsorption, and so on. [7,8]. However, these advanced techniques are ineffective in the treatment of solutions with very low metal concentrations (1–100 mg L^{-1}). Technological processes give efficient results under conditions where the

---

* Corresponding author.

concentration of metal ions is high and also cause high costs. In addition, high chemical substances, expensive devices, and high energy are required in the treatment processes using these techniques. As a result of these processes, there are disadvantages such as toxic sludge formation [9,10]. The most important disadvantages are the fact that chemical precipitation produces toxic chemical treatment sludge and that operating costs are very high by requiring continuous chemicals. Because reverse osmosis and ion exchange requires high investment and operating costs as well as experienced personnel to control processes, the use of these methods is also very limited [11–13]. Among these methods, removal of heavy metals from water using the adsorption method with low-cost adsorbents can be both economical and effective [14–16]. Activated carbon is the most commonly used adsorbent due to its ease of use and economic efficiency in adsorption. The properties that make the activated carbon so important are a great variety of advanced pore structure and the surface area that can reach very high values [12]. These properties may vary depending on the raw material and production conditions of the activated carbon in the artificial adsorber class. It is possible to obtain activated carbon from all carbonaceous materials. However, the type of raw material used, activation means, and activation conditions determine the end product properties [17]. The number of studies on the use of many biomass waste such as hazelnut husk, apricot kernel, corn cob, olive kernel, rice stalk, apple shell, acorn shell in the production of activated carbon is quite high [3,18–21].

In this study, the removal of chromium(VI) ions from aqueous solutions were realized in batch adsorption systems by activated carbon (AC) adsorbent which was produced at a reasonable price by chemical activation of chestnut inner shells with H_3PO_4. The effect of pH, adsorbent concentration, initial chromium concentration, and temperature on the adsorption of chromium(VI) was investigated. In addition, Cr(VI) adsorption equilibrium, kinetic, and thermodynamic studies were also evaluated.

2. Materials and Methods

2.1. Chemicals

The chemicals used in this study are 0.1 M HCl, 0.1 M NaOH for pH adjustment of the solutions, H_3PO_4, 1.5 diphenyl carbazide, C_3H_6O for use during the experiment and were obtained from Merck Company (Darmstadt, Germany). In the experiments, the Cr(VI) element was used in the experimental study without any purification by purchasing a certified high-purity standards reference material with a concentration of 1,000 mg L^{-1}. All chemicals used in the experiments are of analytical purity and freshly prepared for experimental studies. They are prepared by diluting with deionized water (chemical resistance: 18 MΩ cm).

2.2. Preparation of AC

Wild chestnut inner shell (WCIS) that were used in the study were collected around the Sakarya/Turkey region. WCIS were washed once for the removal of the pollution and then dried in the oven for 24 h at 105°C. In this study, phosphoric acid (H_3PO_4) with an impregnation (H_3PO_4:WCIS) ratio of 1:1 was utilized for the chemical activation of wild chestnut inner shell. The mixture of WCIS and H_3PO_4 were stirred at 70°C for 120 min. on magnetic stirrer and an activation was achieved. The solid samples were separated from the mixture by filtration with blue band filter paper and dried in a drying-oven at 105°C for 24 h. Carbonization was carried out in the tubular reactor (Protherm PTF 12) at an activation temperature of 600°C and under inert nitrogen gas (150 cm^3 min^{-1}). After the carbonization temperature reached the desired maximum temperature, the system was allowed to cool to room temperature. The filtered samples were allowed to dry at 90°C for 24 h. The dried samples were washed thoroughly with distilled water and then heated in a beaker with 1.0 M 100 mL HCl solution for 30 min and washing was continued until the pH value was 7.0 [22].

2.3. Characterization studies

Brunauer–Emmett–Teller (BET) surface area and pore measurements of AC were carried out with MICROMERITIC (Norcross, Georgia, USA) brand ASAP a 2020 surface area meter. In the analysis of the functional groups of activated carbon before and after adsorption, SHIMADZU IR Prestige (Kyoto, Japan) 21 unit brand Fourier transform infrared (FT-IR) (with attenuated total reflectance (ATR) method) spectrometer was used. Absorbance values of functional groups in the structure of 4,000–400 cm^{-1} wavelength range were determined and the structure was tried to be illuminated. Scanning electron microscopy (SEM) analyzes were performed for pre- and post-adsorption of AC. The analyzes were performed on Jeol JSM-6060 LV device and under high vacuum at 20 kV. In order to ensure the conductivity of the powdered AC, gold coating was carried out and this was followed by SEM at 1,000×–300,000× magnification and resolution range of 50 μm–200 nm. X-ray diffraction (XRD) device with brand X-ray diffractometer (Rigaku) was used for qualitative structure analysis of AC before and after adsorption. The sample was analyzed at positions between 10° and 80° 2θ.

2.4. Chromium(VI) analysis

Cr(VI) concentration was determined in UV spectrophotometry via complexation method with 1–5 diphenyl carbazide [23]. 0.5 g of 1–5-diphenyl carbazide was dissolved in 100 mL of acetone. 5 mL solution was taken among solutions and put into the 100 mL volumetric flask for Cr(VI) analysis. Then 25 mL 0.2 N HCl and 2 mL 1–5 diphenyl carbazide solution were added and completed with distilled water to 100 mL, respectively. To prepare Cr(VI) solutions, a stock solution of 1,000 mg L^{-1} was first prepared. The solution prepared at a concentration of 1,000 mg L^{-1} was diluted with deionized water and stock solutions at 1–50 mg L^{-1} concentration were obtained. Absorbance values were measured at 540 nm wavelength after waiting 10 min for color improvement by using glass vessel.

2.5. Adsorption and desorption studies

To the solutions was added 0.1 g of AC, stirred for 60 min at 150 rpm in the shaker. The equilibrated mixture was filtered with blue band filter paper and the adsorbent and solution are separated. Cr(VI) ion concentration in equilibrium in solution phase was determined by measuring with UV visible spectrometer device at a wavelength of 540 nm. All experimental studies were done 3 times and the mean values were taken. The effect of the parameters such as adsorption initial pH (1.0–8.0), initial Cr(VI) concentration (25–250 mg L^{-1}), adsorbent content (0.05–1.0 g 100 mL^{-1}), temperature (293–313 K), and contact time (5–120 min.) was researched. 0.1 M NaOH and 0.1 M HCl were used for pH adjustment. The amount of material adsorbed by the unit mass of the adsorbent is a function of temperature, concentration, pressure, or equilibrium pressure at the moment the system is stabilized during the adsorption process. The equilibrium concentration of Cr(VI) in the solution and the removal percentage were calculated using Eqs. (1) and (2):

$$q_e = \frac{\left(C_0 - C_e\right)}{m} \times V \tag{1}$$

$$\text{Removal}\left(\%\right) = \frac{\left(C_0 - C_e\right)}{C_0} \times 100 \tag{2}$$

where q_e is equilibrium concentration of adsorbed Cr(VI) onto AC (mg g^{-1}). C_0 and C_e are initial (mg L^{-1}) and equilibrium concentration of Cr(VI) in the solution at equilibrium time (mg L^{-1}), respectively. V and m are solution volume (mL) and weight of the adsorbent (g), respectively.

The research of reusability of AC was carried of adsorption of Cr(VI) under specific optimal conditions four times. Before reuse AC containing Cr(VI) was stirred at 298 K and 150 rpm for 3 h with 0.2 M HNO_3 and dried with vacuum at 60°C for 24 h for reactivation.

2.6. Analyses

After adsorption experiments, the solution was passed through a 0.45 µm pore diameter membrane filter (Sartorius, Germany). The concentration of Cr(VI) remaining in the solution was measured according to the Standard Methods by the diphenyl carbazide method in the filtrate [23]. Colorimetric Cr(VI) measurements were performed using Hach Lange DR 6000 UV-visible model spectrophotometer.

3. Results and discussion

3.1. Chemical and morphological characterization results

The surface area and pore distribution of AC are the most important characteristics that determine the adsorption behavior. Results on the surface area AC used in the adsorption study are shown in Table 1.

Table 1
Structural parameters of AC

Textural parameter	AC
BET surface area (S_{BET}) (m^2 g^{-1})	508.00
Langmuir surface area (m^2 g^{-1})	746.46
Micropore area (m^2 g^{-1})	447.71
BJH average pore width (4V A^{-1}) nm	50.71
t-plot outer surface area (m^2 g^{-1})	60.58

Since adsorption is a surface event, the magnitude of adsorption is proportional to the specific surface area. It is desirable that the adsorbed has a large surface area, pore volume, a certain pore distribution, and a particulate structure. Since the increase in the adsorbent concentration will increase the surface area, the amount of adsorbed metal in the unit adsorbent mass increases [24].

The structural changes caused by AC before and after adsorption were investigated by FT-IR analysis. The FTIR spectra of both samples are given in Fig. 1.

Fig. 1 shows the FT-IR spectrum of AC before and after adsorption. According to these spectra, peaks seen in the band of approximately 3,230.89 cm^{-1} indicate the presence of the OH$^-$ tension band alcohol, phenol, or carboxylic acids [24]. The peak seen in 1,740 cm^{-1} band was formed by the effect of olefinic C=C vibrations in aromatic structures. The lignin of chestnut shell is composed of aromatic structures. The peak seen in 1,002.23 cm^{-1} band formed as a result of C–OH stretching. The peak also supports the presence of lignin [25,26]. As shown in Fig. 1b, the peak seen in 3,230.89 cm^{-1} band causes the release of volatile chemicals such as acetic acid and methanol as a result of H_3PO_4 dehydration. In addition, H_3PO_4 caused many aliphatic and aromatic species in the structure of the raw material to break and be released. Carbonization removes the oxygen in the raw material and breaks the aromatic structures in the raw material and transforms it into a cross-linked and more robust carbon-weighted structure [24].

Surface morphology of AC before and after Cr(VI) adsorption was examined by SEM. SEM images (Fig. 2a) show the surface structure of the activated carbon. It is supported by SEM images of activated carbon after Cr(VI) adsorption in the (Fig. 2b).

When it is taken a look at the SEM photographs in Fig. 3a, the surface of AC activated with H_3PO_4 is porous and homogeneous. In the SEM image, the fact that the material has a structure with pores and voids occur as the result of H_3PO_4 evaporation during the carbonization phase [3]. The SEM photographs in Fig. 3b show

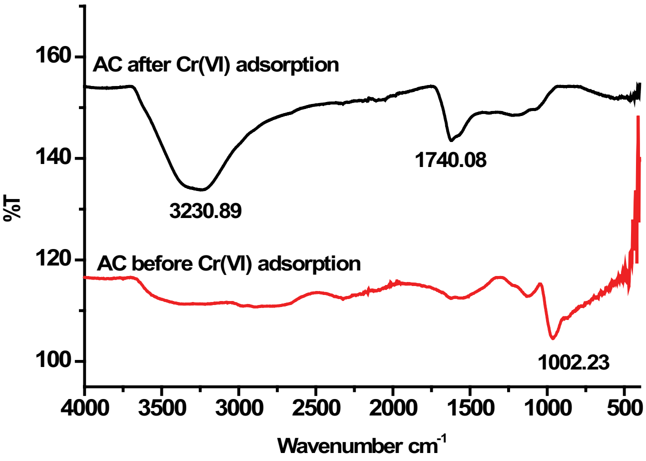

Fig. 1. FTIR spectra of AC before and after Cr(VI) adsorption.

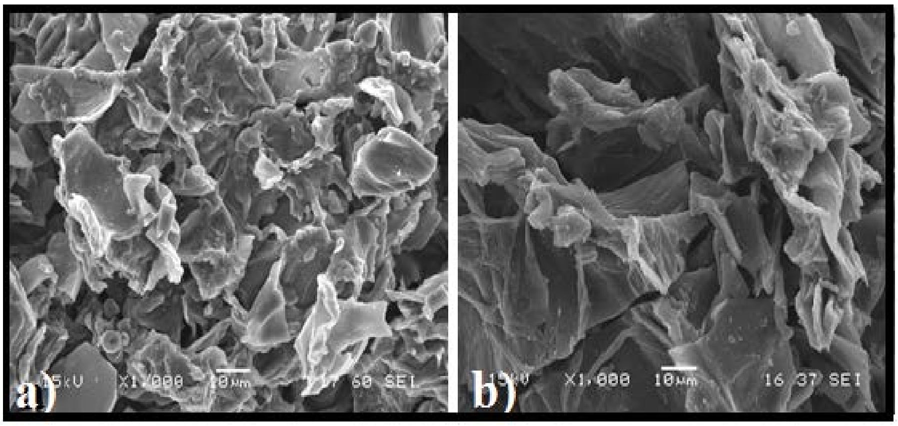

Fig. 2. SEM photographs (10 μm) (a) AC before and (b) AC after Cr(VI) adsorption.

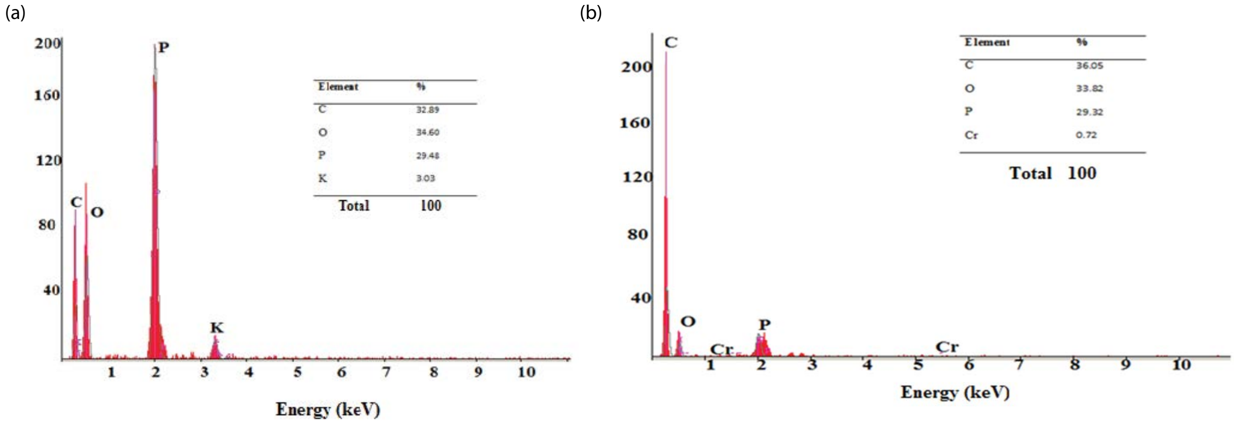

Element	%
C	32.89
O	34.60
P	29.48
K	3.03
Total	100

Element	%
C	36.05
O	33.82
P	29.32
Cr	0.72
Total	100

Fig. 3. SEM/EDS image (a) before Cr(VI) adsorption of AC and (b) Cr(VI) of AC after adsorption.

heterogeneous appearance of AC after Cr(VI) adsorption. This shows us that Cr(VI) adsorption on AC occurs.

Fig. 3a shows the SEM/EDS image of the sample of activated carbon. In Fig. 3b, the adsorption of Cr(VI) was confirmed by energy-dispersive X-ray spectroscopy (EDS) analysis. Fig. 3a shows the pre-adsorption of the peaks of the different elements on the surface of the AC and the EDS analysis after Cr(VI) adsorption. The different peaks shown in Fig. 3b show Cr(VI) adsorbed onto the surface of the AC. As shown in the EDS graphic given in Fig. 3b, C is found with 32.89% and O with rate of 34.60% at the highest rate on the surface of AC adsorbent. Element C and O are formed as a result of the activation of chestnut inner shells. P occurs as the result of activation of activated carbon with H_3PO_4. Similar results are seen in the literature [27].

Fig. 4 shows the XRD spectrum of AC before and after adsorption. Although no characteristic peak is observed in the Fig. 4, peaks of 26° and 44° belong to AC. The structure is generally seen as amorphous. There are studies in the literature that AC is amorphous [21,28].

3.2. *pH effect on Cr(VI) removal yield*

Solution pH, Cr(VI) is one of the important process parameters that effects the adsorption on the adsorbent significantly. In order to determine the effect of initial pH (1.0–8.0) in the removal of Cr(VI) by AC, a study was carried out with 0.1 g adsorbent at a concentration of 250 mg L^{-1}, at 293 K temperature and with 60 min contact time.

Fig. 5 exhibits the higher removal of Cr(VI) ions occurred in the acidic pH value. When pH graphic was looked at, it was seen that adsorption was high in acidic pH (1.0–2.0), removal percentage is almost 99.99%. The intensity of the metal adsorption may be connected to type of functional groups on the adsorbent surface, ionic status and pH of the solution depending on the chemistry of the metals substantially [18,19]. High adsorption of Cr(VI) ions at low pH, may be an expected result due to the existence of Cr(VI) ion at different shape and dimensions in the acidic environment and this may be suitable to nature of the adsorbed surface in the acidic environment. Dominant Cr(VI) ion types in acidic pH, only CrO_4^{2-} is stable on $HCrO_4^-$ and $Cr_2O_7^{2-}$ and neutral pH. Adsorbent surface has become saturated with protons under acidic conditions and supports the adsorption of Cr(VI) ions in anionic form. As the pH of the solution increases, the degree of proton at the surface gradually decreases and this case causes the absorption of Cr(VI) ions. Moreover, as the pH increases there is a challenge between OH^- and CrO_4^{2-} ions, the first one is the dominant type at basic pH value. The decrease in

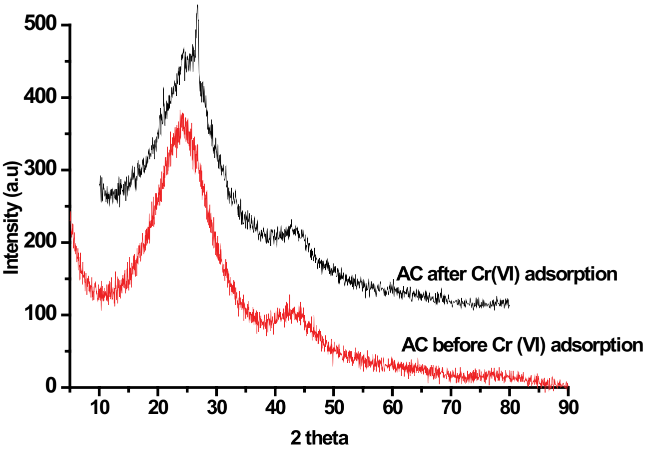

Fig. 4. XRD diffraction profiles AC before and after Cr(VI) adsorption.

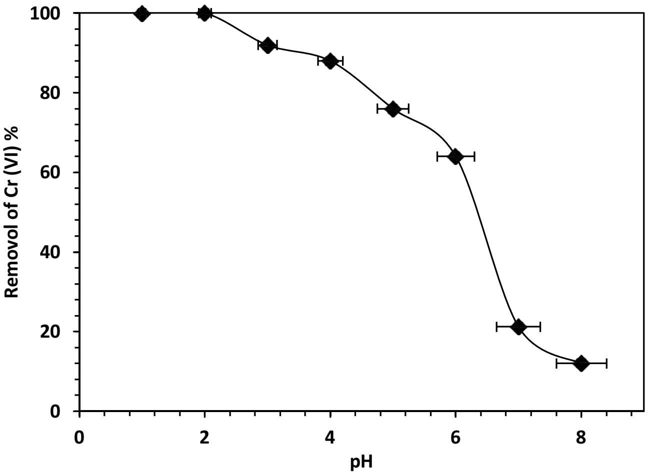

Fig. 5. Effect of pH on the adsorption of Cr(VI) onto AC (C_0 = 250 mg L^{-1}; T = 293 K; dosage = 0.10 g L^{-1}; 150 rpm mixing speed).

net positive surface loads on the adsorbent surface, weakens the electrostatic forces between Cr(VI) ions and adsorbents and causes a decrease at adsorption capacity finally [29]. Due to this effect, adsorption efficiency increases at pH 2.0. After pH 5, the adsorption efficiency decreases gradually due to the increase of OH^- ions in the solution. In our study, Cr(VI) adsorption was higher in adsorption at acidic pH. Subsequent studies were continued with optimum pH of 2.0. In literature, there are many studies in which the pH of Cr(VI) adsorption is 2.0 [3,29,30].

3.3. Mixing speed effect on Cr(VI) removal yield

The effect agitating speed on the removal of the Cr(VI) ion with AC was examined. Removal graphic at 50–250 rpm agitating speed is presented in Fig. 6.

It has seen in the Fig. 6, that agitating speed of removal yield was increased from 50 to 150 rpm and it remained stable. This increase was caused by the increase rate and it was observed that it was used in order to provide surface binding for ion intake improved at 150 rpm shake rate the diffusion of ions to the adsorbent surface. Optimum value of agitating was used as 150 rpm for the other experiments of our study.

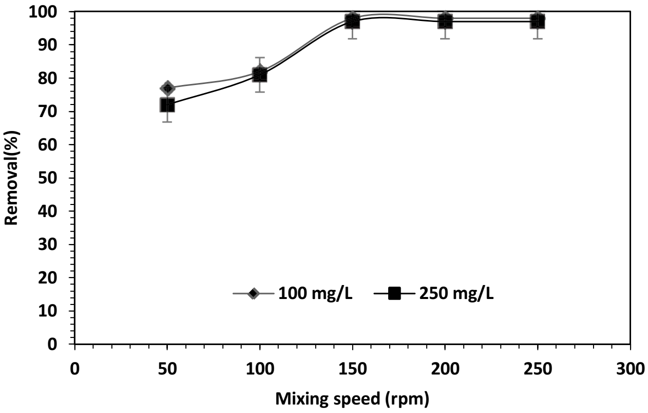

Fig. 6. Effect of agitation speed on removal of Cr(VI) by AC (pH: 2.0; C_0: 100 and 250 mg/L; temperature: 293 K; dosage: 0.1 g 100 mL^{-1}).

3.4. Contact time effect on Cr(VI) removal yield

One of the most important parameters to be examined in order to talk about adsorption efficiency is contact time [31]. In this study, different contact times and metal removal rates obtained against time were determined by keeping all other parameters constant. 0.1 g of adsorbent was mixed with Cr(VI) with a concentration of 100 and 250 mg L^{-1} with a pH of 2.0 by applying different contact times and a graph of adsorption efficiency against time was obtained. Fig. 6 shows the contact time graph for two different concentrations.

Fig. 7 shows that the amount of adsorbed metal increases with contact times up to 30 min, but there is no significant difference in measurements after 30 min and is at a negligible level. A similar trend in hexavalent chromium adsorption as a function of initial Cr(VI) concentration was reported by Ullah et al. [32] (natural and mobilized sugarcane bagasse waste), Hyder et al. [33] (bone char). In the subsequent studies, the optimum contact time was determined as 60 min and the studies were continued with this contact time.

3.5. Adsorbent dosage effect on Cr(VI) removal yield

Determining the appropriate amount of adsorbent in adsorption studies is important in terms of process efficiency and cost. In addition, the excess or lack of functional groups at the surface binding points of the adsorbent plays an important role in the removal of target metals [34]. In our study, a series of experiments were carried out with Cr(VI) solutions at different concentrations of 100 and 250 mg L^{-1} and different amounts of adsorbents and, as a result of that, the effect of changing adsorbents on Cr(VI) adsorption was investigated.

As shown in Fig. 8, the dose amount (between 1 and 5.0 g 100 m L^{-1}) was studied. In the quantity study, the %

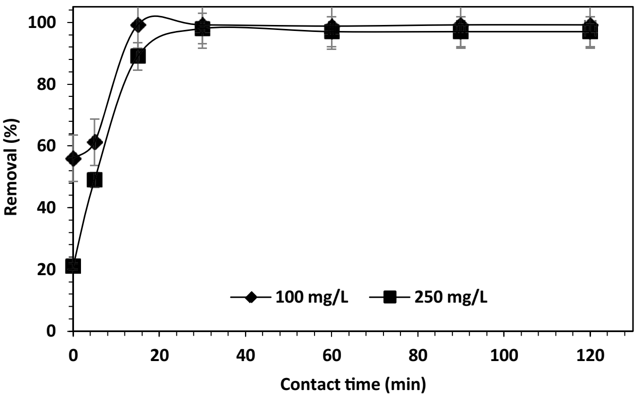

Fig. 7. Effect of contact time on Cr(VI) removal by for AC (pH: 2.0; C_0: 100 and 250 mg L^{-1}; stirring speed: 150 rpm; temperature: 293 K; dosage: 0.1 g 100 mL^{-1}).

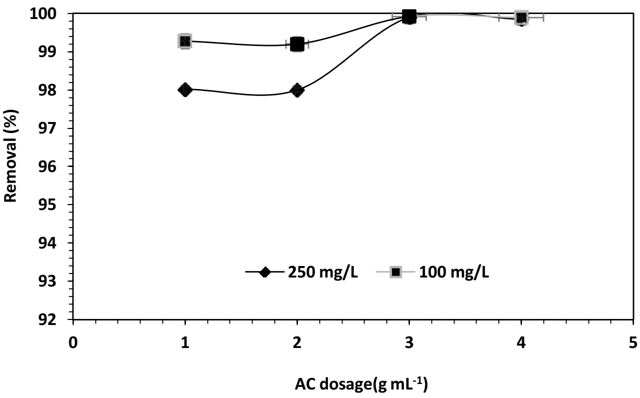

Fig. 8. Effect of AC dose on Cr(VI) removal (pH: 2.0; C_0: 100 and 250 mg L^{-1}; stirring speed: 150 rpm; temperature: 293 K).

removal rate is between 97.00% and 99.82%. Increasing the amount of adsorbent also increases the adsorbent surface area and the number of present binding sites. As a result, it leads to increase in % of adsorbate [35]. In our study, as the increase in mass amount did not affect the change much, the study was continued with 1.0 g as the optimum amount.

3.6. Initial Cr(VI) concentration effect on Cr(VI) removal yield

In order to investigate the removal of initial Cr(VI) concentration, a concentration study was carried out with data obtained as a result of studies with a concentration of 25–250 mg L^{-1} in the range of pH: 2.0, at temperature 293 K and the amount of substance 0.1 g 100 mL^{-1}. Fig. 9 shows the effect of initial concentrations on removal efficiency.

As shown in Fig. 9, the percentage of removal of Cr(VI) decreases with increasing concentration. According to the situation observed here, it shows that the amount of adsorption of Cr(VI) removal here varies depending on the initial concentration. Similarly, in another study [29], researchers found that as the initial chromium(VI) concentration increased, adsorption capacity decreased.

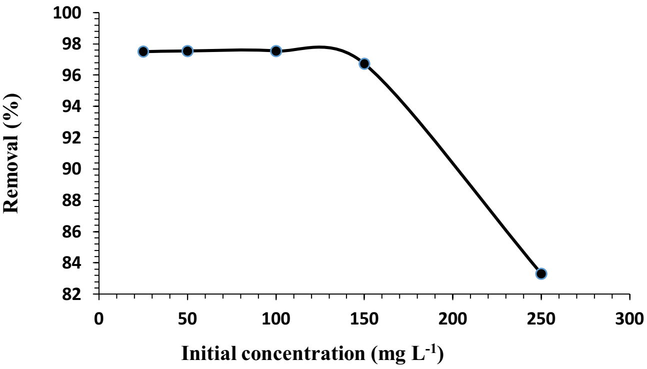

Fig. 9. Effect of initial concentrations on Cr(VI) removal efficiency (pH: 2.0; temperature: 293 K; adsorbent dosage: 0.1 g 100 mL^{-1}).

3.7. Adsorption kinetics

Adsorption kinetics is used to determine which mechanisms adsorbed material fits during adsorption to the adsorbent surface [36]. In this study, two different kinetic models were used to determine Cr(VI) adsorption on AC. Adsorption kinetics is explained by pseudo-first and second-order equations. The pseudo-first (and pseudo-second-order equation formulations are shown below [Eqs. (3) and (4)].

Pseudo-first-order equation formulation [37]:

$$\ln\left(q_e - q_t\right) = \ln q_e - k_1 t \tag{3}$$

where q_e is the amount of adsorbed material per gram of adsorbent at equilibrium (mg g^{-1}); q_t is the amount of adsorbed material per gram of adsorbent at any given time (mg g^{-1}); t is the contact time (min.); k_1 is the rate constant (1 dk^{-1}).

Pseudo-second-order equation formulation [38]:

$$\frac{t}{q_t} = \frac{1}{k_2 q_e^2} + \frac{t}{q_e} \tag{4}$$

where k_2 is the pseudo-second-order equation constant (g mg min^{-1}); t is the specified time constant (min); q_t is the amount of adsorbed material at the end of the t period (mg g^{-1}); q_e is the amount of adsorbed material in equilibrium (mg g^{-1}).

The linearity of the kinetic model is very important in determining which kinetic model is suitable for the adsorption system (Figs. 10 and 11).

q_e values obtained from results, calculated speed constants, and correlation coefficients are shown in Table 2.

Parameters of the pseudo-first-order and the pseudo-second-order for Cr(VI) adsorption.

Experimental and theoretical q_e values, calculated speed constants, and correlation coefficients are listed in Table 2. The linearity of the kinetic model is very important in deciding the model suitable for the adsorption system. As can be seen from the kinetic studies for both concentrations, the R^2 values of the second-order equation are higher than the R^2 value of the first-order equation. The second criterion for deciding which kinetic model describes the

Table 2
Parameters of the pseudo-first-order and the pseudo-second-order for Cr(VI) adsorption

			Pseudo-first-order			Pseudo-second-order		
Sample	C_0 (mg L^{-1})	$q_{e,\text{exp}}$ (mg g^{-1})	k_1 (min^{-1})	$q_{e,\text{cal}}$ (mg g^{-1})	R^2	k_2 (g mg^{-1} min^{-1})	$q_{e,\text{cal}}$ (mg g^{-1})	R^2
AC	100	98.76	0.06	24.53	0.70	0.83	100.0	0.99
AC	250	248.78	0.18	60.94	0.76	1.73	250.0	0.99

adsorption system is the proximity of experimental and theoretical q_e values. The pseudo-second-order equation found these values closer than the first-order equation. As a result, Cr(VI) adsorption was found to be compatible with the second-order equation. Similar approaches have been made in the literature for Cr(VI) removal studies from AC and aqueous solutions [16,21,39].

3.8. Adsorption isotherms

Isotherm study for Cr(VI) removal with AC was carried out at 293 K temperature, pH: 2.0, contact time of 60 min, 150 rpm mixing speed, and 25–250 mg L^{-1} initial concentrations. In order to determine the suitability of these data to isotherm model, the relationship between equilibrium concentration and C_e/q_e should be determined. This relationship is explained by the equation given in Fig. 12 and curve formation, and then isotherm constants are obtained from the slope and shift values of the curve. In these equations, q_e represents the amount of metal adsorbed by the adsorbent (mg g^{-1}) and C_e represents to the concentration of metal in equilibrium (mg L^{-1}). The analysis of adsorption data when equilibrium is reached is important for the optimization of the adsorption process. For this purpose, how the adsorption changes by using the data obtained from different studies has been examined with the help of different adsorption isotherms [40,41]. The linear formulation of this model can be given as follow:

$$\frac{C_e}{q_e} = \frac{1}{q_m K_L} + \frac{1}{q_m} C_e \quad (5)$$

where C_e is the concentration of the substance remaining in the solution after adsorption (mg L^{-1}), q_e is the amount of substance collected on the unit adsorbent (mg g^{-1}), K_L is the isotherm constant (L mg^{-1}), q_m is the maximum adsorption capacity of adsorbent (mg g^{-1}). The amount of adsorbed material obtained as a result of adsorption and Freundlich isotherm graphs obtained by using Eq. (6), Freundlich equation are given. Here, K_f and n constants are calculated by using the equation with the appropriate parameters.

Freundlich isotherm is given by the following equation:

$$\ln q_e = \ln K_f + \frac{1}{n} C_e \quad (6)$$

where q_e is equilibrium concentration (mg g^{-1}) of adsorbate onto surface of adsorbent, C_e is adsorbate (mg L^{-1}) in solution, K_f and n are Freundlich's constants. These calculated values are shown in Table 3.

The maximum adsorption capacity q_m and Langmuir constant K_L were calculated according to the slope and intersection points in the graphs and the data obtained when calculated by taking the appropriate parameters from the graphs and by using the equations at Eq. (5) are shown in Table 3.

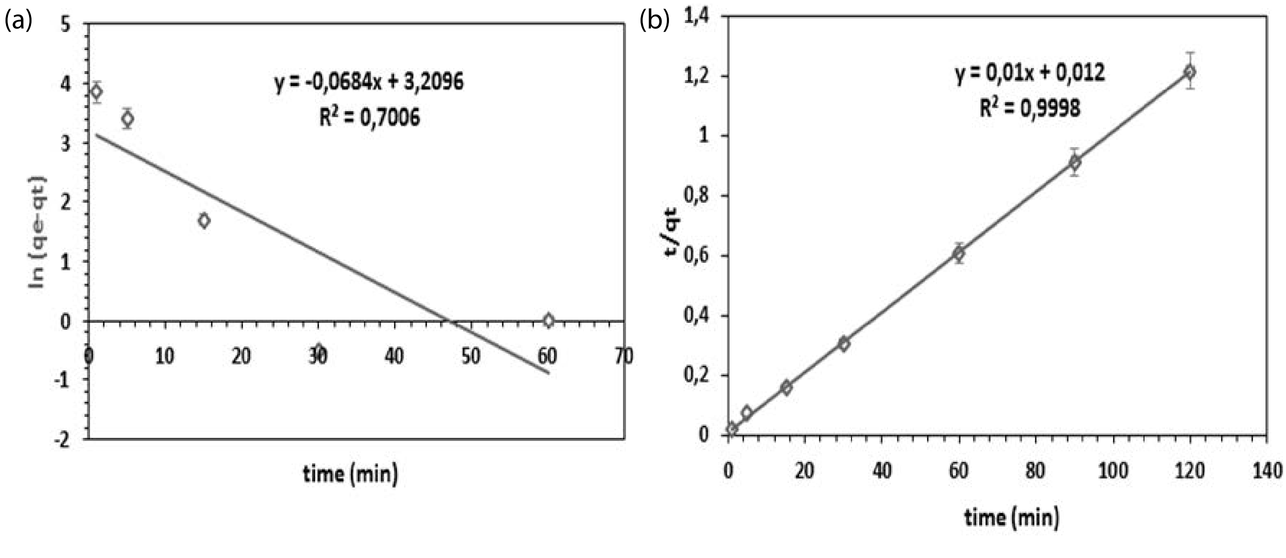

Fig. 10. (a) Pseudo-first-order kinetics of the adsorption of Cr(VI) onto AC and (b) pseudo-second-order kinetics of the adsorption of Cr(VI) onto AC (Cr(VI) concentration 100 mg L^{-1}; dosage 0.1 g; pH = 2.0, 60 min).

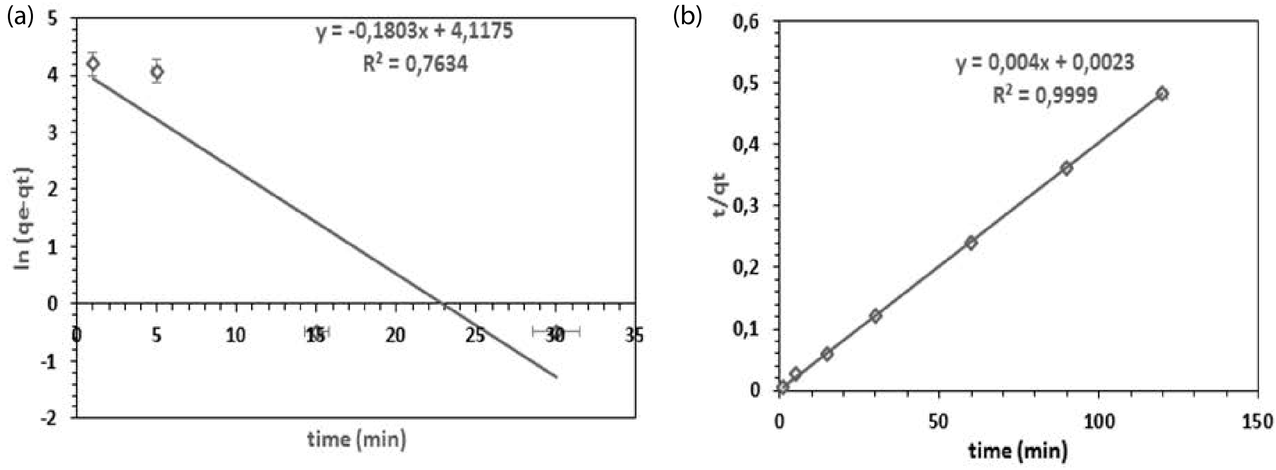

Fig. 11. (a) Pseudo-first-order kinetics of the adsorption of Cr(VI) onto AC and (b) pseudo-second-order kinetics of the adsorption of Cr(VI) onto AC (Cr(VI) concentration 250 mg L^{-1}; dosage 0.1 g; pH = 2.0, 60 min).

Table 3
Langmuir and Freundlich isotherm constants

Temperature (K)	Sample	Langmuir isotherms			Freundlich isotherms		
		q_m (mg g^{-1})	b (L mg^{-1})	R^2	K_F	n (L mg^{-1})	R^2
293	AC	227.27	0.25	0.99	42.09	2.12	0.91

It can be said that correlation coefficient (R^2) value is suitable for Langmuir isotherm because of high correlation value when the experimental data obtained is taken into consideration. It is seen that Langmuir isotherm compatible adsorbent surface is homogeneous and the surface is covered with a single layer. Among the Langmuir constant values, q_m, which expresses adsorption capacity, was found to be highest at 293 K and q_m = 227.27 mg g^{-1} and K_L value for adsorption energy was found to be K_L = 0.25 L mg^{-1}.

3.9. Effect of temperature on Cr(VI) yield

In order to determine the effect of temperature on the adsorption of Cr(VI), 60 min experiments were performed with 100 mL of adsorbate solution at pH 2.0 and 0.1 g adsorbent at three different temperatures (293–313 K). Fig. 13 shows the effect of temperature on Cr(VI) adsorption.

The effect of temperature on Cr(VI) adsorption is shown. It is seen that Cr(VI) adsorption increases with increasing temperature, which indicates that Cr(VI) adsorption is endothermic.

3.10. Thermodynamic parameters of adsorption

Fig. 14 shows the graph plotted between lnK_d and 1/T for three different temperatures. During the adsorption, enthalpy, entropy, free enthalpy change, and equilibrium constant are determined and the adsorption event is examined thermodynamically. One of the important parameters to determine the thermal properties of the adsorption process is temperature. In this study, 0.1 g AC and AC 100 and 250 mg L^{-1} concentration of Cr(VI) solutions were used, equilibrium times were carried out at three different temperatures (293, 303, and 313 K) and the effect of different temperature changes on Cr(VI) adsorption was studied. Fig. 14 shows the effect of temperature on Cr(VI) adsorption. In this respect, the adsorption equilibrium constants (K_d) are plotted in response to 1/T values as shown in Fig. 14.

$$\Delta G^\circ = -RT \ln K_d \tag{7}$$

$$\ln K_d = \frac{b_2}{b_1} \tag{8}$$

As can be seen Fig. 14, adsorption capacities increased due to the increase in temperature. This increase is a clear indication of the endothermic property of adsorption of Cr(VI) to AC adsorbent. Table 4 shows thermodynamic parameters.

When Table 4 is examined, the adsorption data show that $\Delta G^\circ < 0$ values are negative at all temperatures, confirming the spontaneous nature of adsorption. A positive value of $\Delta H^\circ > 0$ indicates that the adsorption process is endothermic. In other words, the applicability of the adsorption process can be understood by the fact that enthalpy and Gibbs free energy are negative. Positive $\Delta S^\circ > 0$ values indicate increased coincidence of adsorbent at the solid–liquid interface during adsorption [24,42]. Whether adsorption occurs spontaneously depends on Gibbs free energy, and negative ΔG° indicates that adsorption is spontaneous [33]. In addition, the increase of ΔG° with increasing temperature indicates that

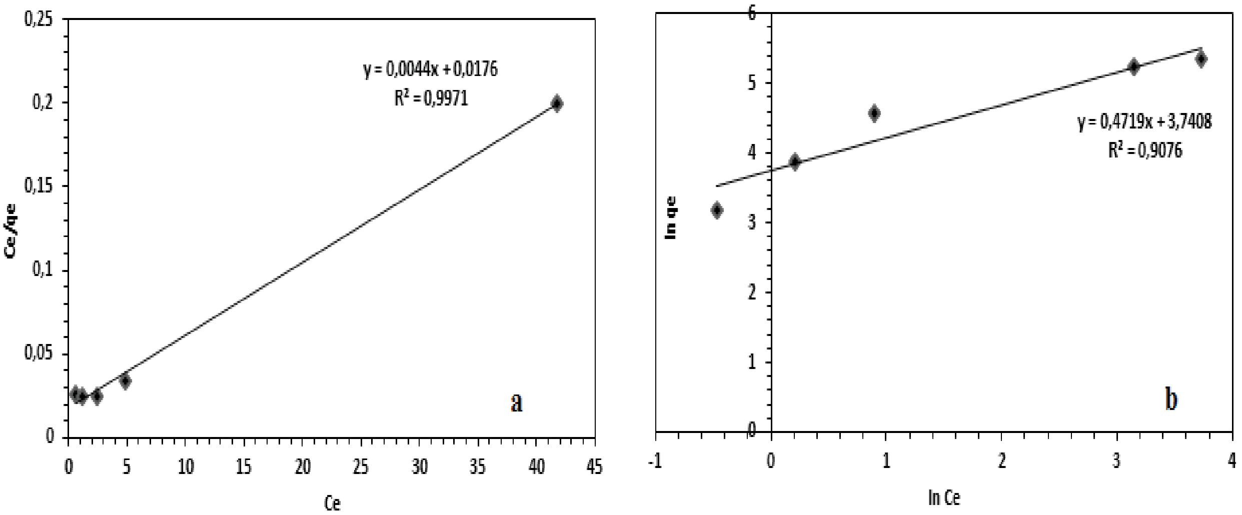

Fig. 12. (a) Langmuir isotherm plots obtained for the adsorption Cr(VI) onto AC sorbent and (b) Freundlich isotherm plots obtained for the adsorption Cr(VI) onto AC sorbent (pH: 2.0; contact time: 60 min; dosage: 0.1 g).

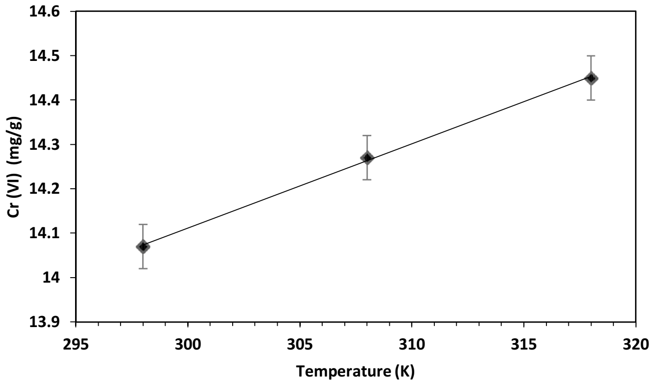

Fig. 13. Effect of temperature on Cr(VI) yield.

Cr(VI) is more adsorbed at higher temperatures. A positive value of $\Delta H°$ indicates that the adsorption is endothermic. Standard entropy values ($\Delta S°$) were found to be positive for all temperatures. A positive value of $\Delta S°$ indicates that there may be a structural change between AC and Cr(VI).

3.11. Reusability

Using more than one adsorbent is economically very important. Fig. 15 showed that the adsorption efficiency for both concentrations was significantly reduced up to three cycles and maintained 74.22% for 100 mg L^{-1} and 75.67% for 250 mg L^{-1} after four cycles.

3.12. Comparison of adsorption capacities for Cr(VI) removal of prepared AC sorbents

Comparison of adsorption capacities in Cr(VI) removal of different adsorbent materials in the literature is shown in Table 5.

The maximum adsorption capacity of the prepared AC adsorbent for Cr(VI) adsorption from aqueous solution was found to be 293 K and 227.27 mg g^{-1} at 0.1 g. Table 5 shows the comparison of adsorption capacities in different sorbents with AC adsorbents in the literature. Considering the data given in the Table 5, it is seen that the adsorbent prepared in our study has higher adsorption capacity than the adsorbents in other studies. Therefore, compared with the other studies in our study, it is thought that AC produced by H_3PO_4 activation from chestnut inner shells is an effective adsorbent for Cr(VI) removal.

4. Conclusions

In this study, AC was prepared from WCIS using H_3PO_4 activation method for the adsorption of Cr(VI) from

Table 4
Thermodynamic parameters of Cr(VI) adsorption

C_0 (mg L^{-1})	T (K)	$\Delta G°$ (kJ mol^{-1})	$\Delta H°$ (kJ mol^{-1})	$\Delta S°$ (J mol K)
	293	–3.31		
100	303	–6.97	63.20	231.03
	313	–10.12		
	293	–3.84		
250	303	–6.82	84.07	303.32
	313	–12.54		

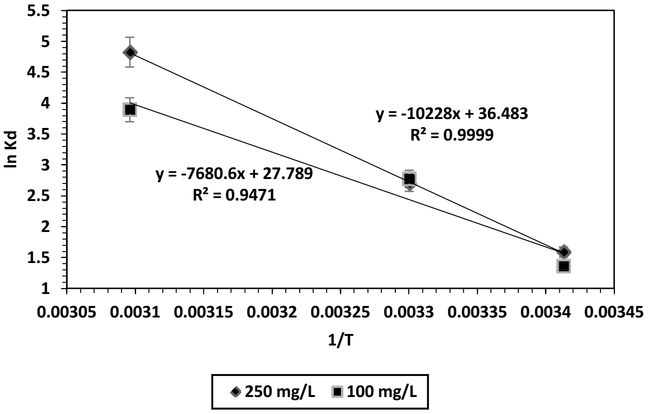

Fig. 14. 1/T graph against lnK_d.

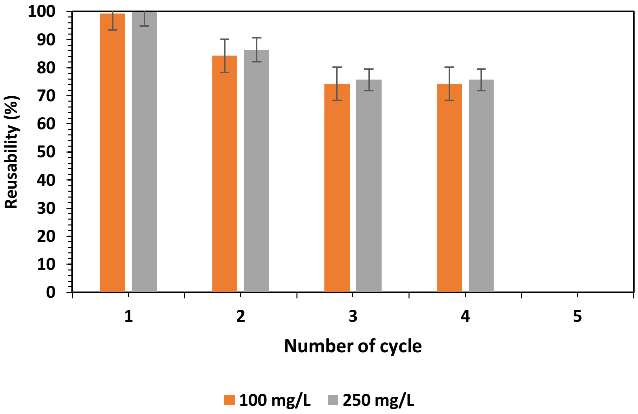

Fig. 15. Effect of number of cycle on Cr(VI) removal yield.

Table 5
Comparison of Cr(VI) adsorption among different adsorbents

Adsorbent	pH	Temperature (K)	Dosage (g mL^{-1})	C_0 (mg L^{-1})	Adsorption capacity (mg g^{-1})	References
Tea waste	7.0	303	0.15/100	100–450	199.52	[6]
Akadama clay	2.0	293	5/1,000	50	4.29	[43]
Coffee wastes	2.0	303–323	2/1,000	10–30	87.72	[44]
Rice straw	2.0	333	2/1,000	100	140.39	[45]
Chitosan	2.0	29	3.22/100	100	112.9	[46]
AC	2.0	293	0.1/100	25–250	227.27	This study

aqueous solutions. Structural analysis of AC before and after adsorption was performed by FTIR, XRD, BET, and elemental analysis by SEM-EDS analysis. Optimum conditions for maximum Cr(VI) removal were found to be pH = 2.0, contact time 60 min, adsorbent content 0.1 g, and suitable temperature as 293 K. As a result of experimental studies, it has been observed that Cr(VI) removal with AC we produce is carried out with high efficiency. In Cr(VI) removal, it was observed that removal of adsorbents increased with increasing amount of adsorbent, whereas Cr(VI) removal decreased with increasing initial metal concentration. The results obtained showed that Cr(VI) adsorption corresponds to Langmuir adsorption isotherm. In our study, the maximum adsorption capacity of Cr(VI) adsorption on AC was found as $q_{\max}$ = 227.27 mg g^{-1}. In the Langmuir isotherm, the fact that the value of R^2 is generally greater than 0.95 ≥ indicates that chemical adsorption (complexation) is more effective. It is thought that AC adsorbent is a suitable adsorbent for Cr(VI) removal due to its high surface area and porosity, natural resource requirement, low cost, and easy production ability.

References

[1] S.M. Gaikwad, C. Balomajumder, Tea waste biomass activated carbon electrode for simultaneous removal of Cr(VI) and fluoride by capacitive deionization, Chemosphere, 184 (2017) 1141–1149.

[2] N.N. Thinh, P.T.B. Hanh, L.T.T. He, L.N. Anh, T.V. Hoang, V.D. Hoang, L.H. Dang, N.V. Khoi, T.D. Lam, Magnetic chitosan nanoparticles for removal of Cr(VI) from aqueous solution, Mater. Sci. Eng., C, 33 (2013) 1214–1218.

[3] I. Enniya, L. Rghioui, A. Jourani, Adsorption of hexavalent chromium in aqueous solution on activated carbon prepared from apple peels, Sustainable Chem. Pharm., 7 (2018) 9–16.

[4] P. Miretzky, A.F. Cirell, Cr(VI) and Cr(III) removal from aqueous solution by raw and modified lignocellulosic materials: a review, J. Hazard. Mater., 180 (2010) 1–19.

[5] R. Gupta, S. Kumar, G. Gomes, C.K. Kuhad, Kinetic study of batch and fed-batch enzymatic saccharification of pretreated substrate and subsequent fermentation toethanol, Biotechnol. Biofuels, 5 (2012) 5–16.

[6] A. Gupta, B. Majumder, Simultaneous adsorption of Cr(VI) and phenol onto tea waste biomassfrom binary mixture: multicomponent adsorption thermodynamic and kinetic study, J. Environ. Chem. Eng., 3 (2015) 785–796.

[7] S.A. Nabi, M. Shahadat, R. Bushra, A.H. Shalla, F. Ahmed, Development of composite ionexchange adsorbent for pollutants removal from environmental wastes, Chem. Eng. J., 165 (2010) 405–412.

[8] M. Najafi, R. Rostamian, A.A. Rafati, Chemically modified silica gel with thiol group as an adsorbent for retentiono some toxic soft metal ions from water and industrial effluent, Chem. Eng. J., 168 (2011) 426–432.

[9] P. Kaewsarn, Biosorption of Copper(II) from aqueous solutions by pre-terated biomass of marine algae *Padina* sp, Chemosphere, 47 (2002) 1081–1085.

[10] Z. Aksu, Ü. Acikel, E. Kabasakal, S. Sezer, Equilibrium modelling of individual and simultaneous biosorption of Chromium(VI) and Nickel(II) onto dried activated sludge, Water Res., 36 (202) 3063–3073.

[11] M. Owlad, M.K. Aroua, W.A.W. Daud, S. Baroutian, Removal of hexavalent chromium-contaminated water and wastewater: a review, Water Air Soil Pollut., 200 (2009) 59–77.

[12] V.K. Gupta, S. Agarwal, T.A. Saleh, Synthesis and characterization of alumina coated carbon nanotubes and their application for lead removal, J. Hazard. Mater., 185 (2011) 17–23.

[13] Z.A. Al-Othman, R. Ali, M. Naushad, Hexavalent chromium removal from aqueous medium by activated carbon prepared from peanut shell: adsorption kinetics equilibrium and thermodynamic studies, Chem. Eng. J., 184 (2012) 238–247.

[14] Y. Wang, L. Shu, V. Jegatheesan, B. Gao, Removal and adsorption of diuron through nanofiltration membrane: the effects of ionic environment and operating pressures, Sep. Purif. Technol., 74 (2010) 236–241.

[15] V.K. Gupta, T.A. Saleh, Sorption of pollutants by porous carbon carbon nanotubes and fullerene-an overview, Environ. Sci. Pollut. Res., 20 (2013) 2828–2843.

[16] S.K. Kumar, T. Gupta, S.S. Kakan, S. Kalidhasan, V.R. Manasi, N. Rajesh, N. Rajesh, Effective adsorption of hexavalent chromium through a three center (3c) co-operative interaction with an ionic liquid and biopolymer, J. Hazard. Mater., 239–240 (2012) 213–224.

[17] R.C. Bansal, M. Goyal, Activated Carbon Adsorption, Taylor and Francis, London, 2005.

[18] R. Tseng, S. Tseng, Pore structure and adsorption performance of the KOH activated carbons prepared from corncob, J. Colloid Interface Sci., 287 (2005) 428–437.

[19] A.A. El-Hendawy, Surface and adsorptive properties of carbons prepared from biomass, Appl. Surf. Sci., 252 (2005) 287–295.

[20] Y. Sudaryanto, S.B. Hartono, W. Irawaty, H. Hindarso, S. Ismadji, High surface area activated carbon prepared from cassava peel by chemical activation, Bioresour. Technol., 97 (2006) 734–739.

[21] E. Altıntıg, M. Onaran, A. Sarı, H. Altundag, M. Tuzen, Preparation characterization and evaluation of bio-based magnetic activated carbon for effective adsorption of malachite green from aqueous solution, Mater. Chem. Phys., 220 (2018) 313–321.

[22] A.A. El Hendawny, S.E. Samra, B.S. Girgis, Adsorption characteristics of activated carbons obtained from corncob, Colloids Surf., A, 180 (2001) 209–221.

[23] APHA, Standard Methods for the Examination of Water and Wastewater, 18th ed., American Public Health Association (APHA), American Water Works Association (AWWA) and Water Pollution Control Federation (WPCF), Washington, DC, 1992.

[24] L. Liu, Y. Lin, Y. Liu, H. Zhu, Q. He, Removal of methylene blue from aqueous solutions by sewage sludge based granular activated carbon: adsorption equilibrium kinetics and thermodynamics, J. Chem. Eng. Data, 58 (2013) 2248–2253.

[25] W. Shen, Z. Li, Y. Liu, Surface chemical functional groups modification of porous carbon, Recent Pat. Chem. Eng., 1 (2008) 27–40.

[26] B.H. Hameed, Evaluation of papaya seeds as a novel non conventional low cost adsorbent for removal of methylene blue, J. Hazard. Mater., 162 (2009) 939–944.

[27] X. Zuo, R. Balasubramanian, Evaluation of a novel chitosan polymer-based adsorbent for the removal of chromium(III) in aqueous solutions, Carbohydr. Polym., 92 (2013) 2181–2186.

[28] T.H. Liou, S.J. Wu, Characteristic of microporous/mesoporous carbons prepared from rice husk under base and acid treated conditions, J. Hazard. Mater., 171 (2009) 693–703.

[29] M.H. Dehghani, D. Sanaei, I. Ali, A. Bhatnagar, Removal of chromium(VI) from aqueous solution using treated waste newspaper as a low-cost adsorbent: kinetic modeling and isotherm studies, J. Mol. Liq., 215 (2016) 671–679.

[30] U.K. Garg, M.P. Kaur, V.K. Garg, D. Sud, Removal of hexavalent chromium from aqueous solution by agricultural waste biomass, J. Hazard. Mater., 140 (2007) 60–68.

[31] E. Malkoc, Y. Nuhoglu, M. Dundar, Adsorption of chromium(VI) on pomace - anolive oil industry waste: batch and column studies, J. Hazard. Mater. B, 138 (2006) 142–151.

[32] I. Ullah, R. Nadeem, M. Iqbal, Q. Manzoor, Biosorption of chromium onto native and immobilized sugarcane bagasse waste biomass, Ecol. Eng., 60 (2013) 99–107.

[33] A.H.M.G. Hyder, S.A. Begum, N.O. Egiebor, Adsorption isotherm and kinetic studies of hexavalent chromium removal from aqueous solution onto bone char, J. Environ. Chem. Eng., 3 (2015) 1329–1336.

[34] J. Yang, M. Yu, W. Chen, Adsorption of hexavalent chromium from aqueous solution by activated carbon prepared from longan seed: kinetics equilibrium and thermodynamics, J. Ind. Eng. Chem., 21 (2015) 414–422.

[35] W. Liu, J. Zhang, C. Zhang, Y. Wang, Y. Li, Adsorptive removal of Cr(VI) by Fe modified activated carbon prepared from trapa natans husk, Chem. Eng. J., 162 (2010) 677–684.

[36] A.C. Martins, O. Pezoti, A.L. Cazetta, K.C. Bedin, D.A.Yamazaki, G.F. Bandoch, T. Asefa, J.V. Visentainer, V.C. Almeida, Removal of tetracycline by NaOH - activated carbon produced from macadamia nut shells: kinetic and equilibrium studies, Chem. Eng. J., 260 (2015) 291–299.

[37] S. Lagergren, Zur theorie der sogenannten adsorption gelöster stofe, Kungl. Sven. Vetenskapsakad. Handl., 24 (1898) 1–39.

[38] Y.S. Ho, G. McKay,Pseudo-second order model for sorption processes, Process Biochem., 34 (1999) 451–465.

[39] S. Karnjanakom, P. Maneechakr, Adsorption behaviors and capacities of Cr(VI) onto environmentally activated carbon modified by cationic (HDTMA and DDAB) surfactants, J. Mol. Struct., 1186 (2019) 80–90.

[40] I. Langmuir, The adsorption of gases on plane surfaces of glass, mica and platinum, J. Am. Chem. Soc., 40 (1918) 1361–1403.

[41] H.M.F. Freundlich, Over the adsorption in solution, J. Phys. Chem. C, 57 (1906) 385–470.

[42] L. Li, F. Liu, H. Duan, X. Wang, J. Li, Y. Wang, C. Luo, The preparation of novel adsorbent materials with efficient adsorption performance for both chromium and methylene blue, Colloids Surf., B, 141 (2016) 253–259.

[43] Y. Zhao, S. Yang, D. Ding, J. Chen, Y. Yang, Y. Lei, C. Feng, Z. Zhang, Effective adsorption of Cr(VI) from aqueous solution using natural Akadama clay, J. Colloid Interface Sci., 395 (2013) 198–204.

[44] W. Cherdchoo, S. Nithettham, J. Charoenpanich, Removal of Cr(VI) from synthetic wastewater by adsorption onto coffee ground and mixed waste tea, Chemosphere, 221 (2019) 758–767.

[45] C. Lin, W. Luo, T. Luo, Q. Zhou, H. Li, L. Jing, A study on adsorption of Cr(VI) by modified rice straw: characteristics performances and mechanism, J. Cleaner Prod., 196 (2018) 626–634.

[46] T. Zhu, W. Huang, L. Zhang, J. Gao, W. Zhang, Adsorption of Cr(VI) on cerium immobilized cross-linked chitosancomposite in single system and coexisted with Orange II in binarysystem, Int. J. Biol. Macromol., 103 (2017) 605–612.